Mesodermal patterning defect in mice lacking the Ste20 NCK interacting kinase (NIK)

Yingzi Xue[1], Xiaozhong Wang, Zhai Li[1], Noriko Gotoh[1], Deborah Chapman[2] and Edward Y. Skolnik[1],*

[1]New York University Medical Center, Skirball Institute of Biomolecular Medicine, Department of Pharmacology, 540 First Avenue, NY, NY10016, USA
[2]University of Pittsburgh, Department of Biological Sciences, Fifth and Ruskin Avenues, Pittsburgh, PA 15260, USA
*Author for correspondence (e-mail: skolnik@saturn.med.nyu.edu)

SUMMARY

We have previously shown that the *Drosophila* Ste20 kinase encoded by *misshapen* (*msn*) is an essential gene in *Drosophila* development. *msn* function is required to activate the *Drosophila* c-Jun N-terminal kinase (JNK), basket (Bsk), to promote dorsal closure of the *Drosophila* embryo. Later in development, *msn* expression is required in photoreceptors in order for their axons to project normally. A mammalian homolog of *msn*, the NCK-interacting kinase (NIK) (recently renamed to mitogen-activated protein kinase kinase kinase kinase 4; Map4k4), has been shown to activate JNK and to bind the SH3 domains of the SH2/SH3 adapter NCK. To determine whether NIK also plays an essential role in mammalian development, we created mice deficient in NIK by homologous recombination at the *Nik* gene. *Nik*$^{-/-}$ mice die postgastrulation between embryonic day (E) 9.5 and E10.5. The most striking phenotype in *Nik*$^{-/-}$ embryos is the failure of mesodermal and endodermal cells that arise from the anterior end of the primitive streak (PS) to migrate to their correct location. As a result *Nik*$^{-/-}$ embryos fail to develop somites or a hindgut and are truncated posteriorly. Interestingly, chimeric analysis demonstrated that NIK has a cell nonautonomous function in stimulating migration of presomitic mesodermal cells away from the PS and a second cell autonomous function in stimulating the differentiation of presomitic mesoderm into dermomyotome. These findings indicate that despite the large number of Ste20 kinases in mammalian cells, members of this family play essential nonredundant function in regulating specific signaling pathways. In addition, these studies provide evidence that the signaling pathways regulated by these kinases are diverse and not limited to the activation of JNK because mesodermal and somite development are not perturbed in *JNK1-, and JNK2-*deficient mice.

Key words: Ste20 kinase, NCK interacting kinase (NIK), *misshapen*, Gastrulation, knockout, N-terminal JUN kinase (JNK), Mouse

INTRODUCTION

Ste20 kinases constitute a large family of protein kinases that are best known for their roles in activating the JNK MAP kinase pathway and in the regulation of the actin cytoskeleton (Kyriakis, 1999). Based on sequence similarity to the kinase domain of the yeast Ste20 kinase protein, two broad families of Ste20 kinases have been identified in mammalian cells and lower organisms, the p21 activated protein kinase (PAK) and the germinal center kinase (GCK) families (Kyriakis, 1999; Manser and Lim, 1999). However, despite the distant homology between their kinase domains, these two kinase families exhibit many differences in both regulation and function. For example, PAKs, unlike GCK family kinases, possess a CRIB motif and therefore bind and are regulated by Rho family GTPases (Burbelo et al., 1995; Martin et al., 1995). In addition, unlike PAKs which have a C-terminal kinase and an N-terminal regulatory domain, GCK family members contain an N-terminal kinase and a C-terminal regulatory domain whose function is distinct from the regulatory domain

of PAK (Kyriakis, 1999; Su et al., 1997). As a result, it has now been proposed to classify PAK and GCK family members into two distinct protein kinase families (Kyriakis, 1999).

At least 20 different GCK family members have been identified in mammalian cells so far. These GCK members can be further subdivided into 5 subgroups based on similarities in sequence, structure and function (Kyriakis, 1999). Although the specific function served by individual GCK members or by subgroups of GCK in mammalian cells is still poorly defined, most studies have focussed on the role of these kinases in activation of the JNK MAP kinase pathway. With respect to JNK activation, GCK family members can be subdivided into two broad groups, group 1 and group 2 (Kyriakis, 1999). Group 1 kinases activate JNK, and include GCK, GCK related (R), hematopoietic progenitor kinase 1 (HPK1) and NIK (Diener et al., 1997; Hu et al., 1996; Pombo et al., 1995; Su et al., 1997). All group 1 kinases share a conserved C-terminal regulatory domain that may function to couple these kinases to downstream MAP kinase kinase kinase (MAP3Ks) (Su et al., 1997). Less is known about the second group of GCK, which

includes Ste20-like oxidant stress activated kinase 1 (SOK1), mammalian sterile20 like 1 and 2 (MST1 and 2) and lymphocyte oriented kinase (LOK) (Creasy and Chernoff, 1995a; Creasy and Chernoff, 1995b; Kuramochi et al., 1997; Pombo et al., 1997). Members of this group contain a C-terminal domain that is significantly different from those of group 1 members and as yet members of this group have not been linked to activation of a signaling pathway (Kyriakis, 1999).

Recent experiments in both *Drosophila* and *C. elegans* have confirmed an essential role for one member of the GCK family, NIK, in both JNK activation and development in a biologically relevant system (Su et al., 1998; E. Hedgecock and X. Zhu personal communication). We have placed the Ste20 kinase encoded by *misshapen* (*msn*), the *Drosophila* homolog of mammalian NIK, genetically upstream of the JNK MAP kinase pathway in *Drosophila* (Su et al., 1998). The failure to activate JNK in *Drosophila* leads to embryonic lethality due to defects in embryonic dorsal closure; in embryos mutant for components of the JNK pathway the lateral epithelial sheets fail to elongate and migrate dorsally (Noselli, 1998). A number of signaling molecules that are critical for stimulating dorsal closure and JNK activation in *Drosophila* can now be ordered on a signaling pathway. Msn likely functions as a MAP kinase kinase kinase kinase (M4K) and activates the JNK pathway by activating a yet to be defined DM3K. A DM3K would likely phosphorylate and activate the JNK kinase encoded by *hemipterous* (*hep*) (Glise, 1995), which in turn phosphorylates and activates *Drosophila* JNK, encoded by *basket* (*bsk*) (Riesgo-Escovar, 1996; Sluss et al., 1996). DJNK phosphorylates and activates DJun, which in turn cooperates with *DFos* to stimulate transcription of *dpp*, a member of the transforming growth factor-β family (Glise, 1997; Hou, 1997; Kockel, 1997; Riesgo-Escovar and Hafen, 1997a; Riesgo-Escovar and Hafen, 1997b). In addition to its role in dorsal closure, Msn also couples Frizzled (Fz) and Dishevelled (Dsh) to JNK activation in the planar polarity pathway; *msn* mutants show defects in epithelial planar polarity in both the eyes and wings due to defective JNK activation (Mlodzik, 1999; Paricio et al., 1999). In *C. elegans*, *mig-15*, the homolog of mammalian NIK and *Drosophila msn*, has also been found to be an essential gene in development. *mig-15* mutants have a number of developmental defects including defects in Q neuroblast migration and muscle arm targeting, although it is not yet clear whether these defects are due to defective activation of JNK (E. Hedgecock and X. Zhu personal communication).

In addition to activating JNK, NIK contains PXXP motifs that mediate its interaction with the SH3 domains of Nck (Nck1; Su et al., 1997). Nck is a ubiquitously expressed protein composed of one SH2 and three SH3 domains (Lehman et al., 1990). Adapter molecules like Nck are proposed to regulate signaling pathways downstream of tyrosine kinases by coupling catalytic subunits, bound to their SH3 domains, to phosphotyrosine-containing proteins that interact with their SH2 domains (Pawson and Nash, 2000; Schlessinger, 1994). Recent experiments in *Drosophila* have shed light on some functions of Nck in mammalian cells and provide evidence that Ste20 kinases are downstream effectors of Nck. A *Drosophila* homolog of mammalian Nck encoded by *dreadlock* (*dock*) is required for correct targeting of photoreceptor axons (Garrity et al., 1996). *Drosophila Pak* has been shown to be one of the

key targets for regulation by *dock* in this pathway and an interaction between Pak and the SH3 domains of Dock is required for Dock regulation of R cell axon guidance and targeting (Hing et al., 1999). We and others have found that Msn also binds the SH3 domains of Dock and that expression of Msn in photoreceptors is also required for the correct targeting of photoreceptor axons (Ruan et al., 1999; Su et al., 2000). In mammalian cells, NCK couples NIK to tyrosine phosphorylated p62 Dok in Eph-stimulated cells, and this interaction is important for the EphB1 and EphB2 receptors to activate NIK kinase activity as well as JNK and integrins (Becker et al., 2000).

Owing to the important roles of *msn, dock* and *mig-15* in *Drosophila* and *C. elegans* development, we determined whether NIK also performs an essential role in mammalian development by creating mice with a targeted disruption of the Nik locus. Mice containing a homozygous loss-of-function of Nik die around E9.5. The most obvious defect in $Nik^{-/-}$ embryos is the failure of mesodermal cells derived from the anterior end of the primitive streak to migrate away from the streak. As a result, $Nik^{-/-}$ embryos are truncated posteriorly and somitogenesis is greatly affected. The most affected embryos have no somites, while less affected mutants have 1-2 pairs of somites, compared to the 10-15 somites found in control littermates. Interestingly, the failure of mesodermal cells to migrate away from the PS is not due to loss of NIK in these cells because chimeric analysis showed that presomitic mesoderm arising from $Nik^{-/-}$ ES cells migrated to the appropriate position in the chimeric embryos. Thus, NIK is most probably required in the PS to regulate the production of factors that are required for proper cell migration. In addition, NIK also acts in presomitic mesoderm to stimulate its differentiation into somites, because $Nik^{-/-}$ ES cells failed to differentiate into dermomyotome in the chimeric embryos. These findings provide the first evidence for an essential function of a Ste20 kinase in mammalian development.

MATERIALS AND METHODS

Gene targeting

A targeted mutation was introduced into the murine *Nik* gene by homologous recombination in embryonic stem cells as described previously (Joyner, 1993). The *Nik* genomic DNA was isolated by screening a 129 mouse genomic library (Stratagene) with the *Nik* cDNA. A 15 kb genomic *Nik* clone containing the 5′ start ATG of *Nik* was isolated, subcloned into Bluescript KS, and a restriction map was constructed. The 5′ homology arm of the targeting vector was the 4 kb *Kpn*I-*Apa*I murine genomic fragment, which was subcloned into targeting vector pPNT (Tybulewicz et al., 1991). The 3′ homology fragment was a 3.5 kb *Sma*I-*Kpn*I genomic fragment. In the final targeting vector an *Apa*I fragment in the *Nik* genomic DNA is deleted and replaced with a PGK.*neo* cassette. This removes part of exon VI and all of exon VII of the kinase domain is removed. These exons encode subdomain VIII and IX in the kinase domain (at amino acid 165 of *Nik*) and therefore the targeted *Nik* allele lacks critical residues that are essential for a functional kinase (Fig. 1). Following electroporation, G418 and gancyclovir-resistant ES clones were selected and successful targeting of the *Nik* locus was determined by PCR (4/300). The primer pairs used for PCR genotyping the 5′ arm are: *Nik* exon primer (sense) 5′-GAGATCAGCAGCCTCTG-TTCCACA-3′ and an antisense primer to the untranslated region in pGK 5′ GAGATCABCAGCCTCTGTTCCACA 3′; for the 3′ arm:

sense primer to pGK promoter 5′ GCTACCGGTGGATGTGGAA-TGTG 3′ and an antisense primer to a *Nik* intron 5′ GCAAGC-GAGTTAAGTTTAGCCTGCAG 3′. Aggregation chimeras between the targeted ES cell and BALB/c morulas were generated and founders were bred to 129Svev mice or outbred to CD-1 mice. Transmission of the targeted ES clone was determined by coat color analysis and genotyping of offspring. The targeted mutation was propagated in a Swiss Webster genetic backgrounds. Mutant *Nik*$^{-/-}$ homozygous embryos were obtained by crossing *NIK*$^{+/-}$ mice and *Nik*$^{-/-}$ mice were determined by their characteristic phenotype or by PCR analysis as described in Fig. 1.

In situ hybridization

Whole-mount embryo in situ hybridization was performed as described using riboprobes as indicated (Swiatek et al., 1994). To section whole-mount stained embryos, after postfixing in 4.0% formaldehyde overnight, embryos were incubated in 30% sucrose/PBS for 2 days. The embryos were embedded in paraffin wax and sectioned at between 10 and 20 μm. Sections were then mounted onto glass slides and after dewaxing were photographed. The probes used for whole-mount in situ staining were *Shh* (Echelard et al., 1993), *Brachyury* (Herrmann, 1991), *Mox1* (Candia et al., 1992), *HNF3β* (Ang et al., 1993), *fgf4*, *Tbx6* (Chapman et al., 1996), *Otx2* (Simeone et al., 1993), *En1* (Davis and Joyner, 1988), *Gbx2* (Bouillet et al., 1995), and *lim1* (Barnes et al., 1994). The NIK probe corresponds to nucleotides 1347-1845 in full length NIK. This region is located between the kinase domain and C-terminal domain and is the region least conserved between NIK and other Ste20 kinases.

Generation of *Nik*$^{-/-}$ ES cells

Nik$^{-/-}$ ES cells were generated from *Nik K*$^{+/-}$ ES cells by culturing in high concentration of G418 (1.4 mg/ml; Mortensen et al., 1992). G418 clones were expanded and genotyped by Southern blot analysis. 2 *Nik*$^{-/-}$ ES cell lines were obtained out of 35 clones examined.

Generation of chimeric mice and β-galactosidase staining

Chimeric embryos were generated by injecting 8 or 14 *Nik*$^{-/-}$ ES cells into ROSA *lacZ*$^{+/-}$ blastocysts. Injected blastocysts were surgically transferred into the uteri of pseudopregnant CD-1 foster mothers and chimeric embryos were dissected at E9.5, fixed and whole-mount stained for β-galactosidase according to standard protocols (Song et al., 1996).

Generation of *TIE2/lacZ:Nik*$^{-/-}$ mice

TIE2/lacZ (*Tek-lacZ*) transgenic mice were obtained from Jackson Labs and have been described previously (Schlaeger et al., 1997). To generate *TIE2-lacZ:Nik*$^{-/-}$ mice, *TIE2-lacZ/TIE2-lacZ;Nik*$^{+/-}$ mice were crossed and embryos were dissected at embryonic day 9.5. Embryos were whole-mount stained for β-galactosidase as described above.

RESULTS

Targeted disruption of the Ste20 kinase NIK in ES cells by homologous recombination

To create mice with a targeted disruption of the Ste20 kinase NIK, we generated the targeting construct pNIK*neo* in the vector pPNT (Tybulewicz et al., 1991). This construct contains 9 kb of NIK genomic sequence in which half of exon 6 and all of exon 7 of the kinase domain are replaced by a PGK*neo* cassette. These exons encode for subdomains VIII and IX of the NIK kinase domain (at amino acid 165 of the NIK protein) and therefore the targeted *Nik* allele lacks residues that are essential for a functional kinase domain. To prevent potential read through transcription from the *PGK* promoter and to introduce

stop codons in all 3 reading frames, *PGK*-neo was cloned in an opposite orientation to that of NIK. This would be predicted to truncate the coding region after subdomain VI of the kinase domain at amino acid 164 of NIK and would disrupt all major isoforms of NIK that have been described (Fig. 1A). We confirmed that *Nik*$^{-/-}$ mice are unlikely to express either a truncated or alternatively spliced NIK protein because northern analysis did not detect binding of a Nik cDNA probe to RNA derived from *Nik*$^{-/-}$ fibroblasts or ES cells, whereas NIK expression was easily detected in wild-type cells (figure 1D). Four ES clones containing a targeted NIK mutation were identified by screening for the 5′ and 3′ insertion sites by PCR and by Southern blot analysis (Fig. 1B and data not shown).

Morula aggregation was performed for three of the four clones with Balb/c mice. All of the clones generated high-degree chimerisms and when crossed with CD-1 mice generated agouti pups indicating germline transmission. Germline transmission was confirmed by both PCR and Southern blot analysis (Fig. 1C and data not shown). In analysis of the mice, identical results were obtained from all three lines and therefore for simplicity the results described are from pooled data from all 3 lines.

Nik$^{-/-}$ mice die embryonically between day 9.5 and day 10.5

All heterozygous progeny were viable and fertile and did not manifest any overt phenotypes. To determine whether *Nik*$^{-/-}$ mice were viable, *Nik*$^{+/-}$ mice were crossed and litters were genotyped 3 weeks after birth. No homozygous *Nik* mutant littermates were present (0/37) as determined by both PCR and Southern blot analysis (Fig. 1C and data not shown). Since no perinatal lethality was observed in these litters, these findings indicate that *Nik* is a recessive embryonically lethal allele.

To determine the point at which *Nik*$^{-/-}$ mice die, embryos from a cross between *Nik* heterozygous mice were dissected at different gestational stages. Analysis of E10.5 embryos revealed that about 1/4 of the decidua were much smaller, very necrotic and were partially resorbed whereas the remaining were phenotypically normal. To genotype the normal and abnormal embryos, embryos were dissected away from maternal tissues and genotyped by PCR (data not shown). This analysis demonstrated that all of the abnormal embryos were *Nik*$^{-/-}$, while the remaining normal embryos were either *Nik*$^{+/+}$ or *Nik*$^{+/-}$ at the expected ratio of 1:2. Thus, these findings, when coupled with the finding that E9.0 *Nik*$^{-/-}$ embryos have a beating heart, indicate that homozygous mutant *Nik* embryos die about 9.5 days after implantation.

To determine whether the expression pattern of NIK may give an insight into the lethality of *Nik* mutants, the expression pattern of *Nik* mRNA in both E7.5 and E8.5 embryos was determined. Whole-mount in situ hybridization revealed that *Nik* transcripts are widely expressed at both time points (figure 1E). The staining for *Nik* mRNA was specific because the same probe did not give a signal in similarly aged *Nik*$^{-/-}$ embryos and a similarly made sense probe did not give a signal in wild-type embryos (data not shown).

Nik mutant embryos are truncated posteriorly and lack somites and presomitic mesoderm

Morphological and histological analysis of E8.5-9.0 *Nik*$^{-/-}$ embryos demonstrated that *Nik*$^{-/-}$ embryos exhibited a distinct

Fig. 1. Targeted disruption of the *Nik* gene. (A) Targeting construct. The top line shows a restriction map of a portion of the *Nik* gene. An *Apa*I fragment, which includes part of exon 6 and all of exon 7, was replaced with the pGK*neo* gene in the targeting vector. The oligos used for PCR screening to verify homologous recombination are shown. (B) PCR analysis of one ES clone that was successfully targeted at the *Nik* locus. Lanes 1 and 2 show that the 5′ arm was correctly targeted and lanes 3 and 4 show that the 3′ arm was correctly targeted. PCR primers shown in A amplified products of 6.8 kb (lane 1) and 4.5 kb (lane 3), both of which were of the size predicted form the restriction map of the *Nik* gene. To confirm the specificity of the PCR product, the amplified DNA in lane 1 was digested with *Kpn*I (lane 2) and DNA in lane 3 was digested with *Eco*RI (lane 4). Both restriction digests yielded fragments of the expected size. (C) Southern analysis of tail DNA from a wild-type mouse (lane 1) and a *Nik*^{+/−} heterozygous mouse (lane 2). Mouse tail DNA was digested with *Eco*RI, and probed with the 5′ *Sma*I, *Kpn*I fragment shown in A. Southern analysis yielded bands of the predicted size of 12 kb for the wild type and 8 kb for the mutant. (D) Northern analysis of *Nik* expression in wild-type (ES^{+/+}) and *Nik*^{−/−} (ES^{−/−}) ES cells and fibroblasts derived from wild-type (fb^{+/+}) or *Nik*^{−/−} (fb^{−/−}) mice. *Nik* mRNA is not expressed in *Nik* mutant fibrobasts or ES cells. (E) Whole-mount in situ hybridization analysis of E7.5 and E8.5 *Nik*^{+/+} embryos stained for *Nik*.
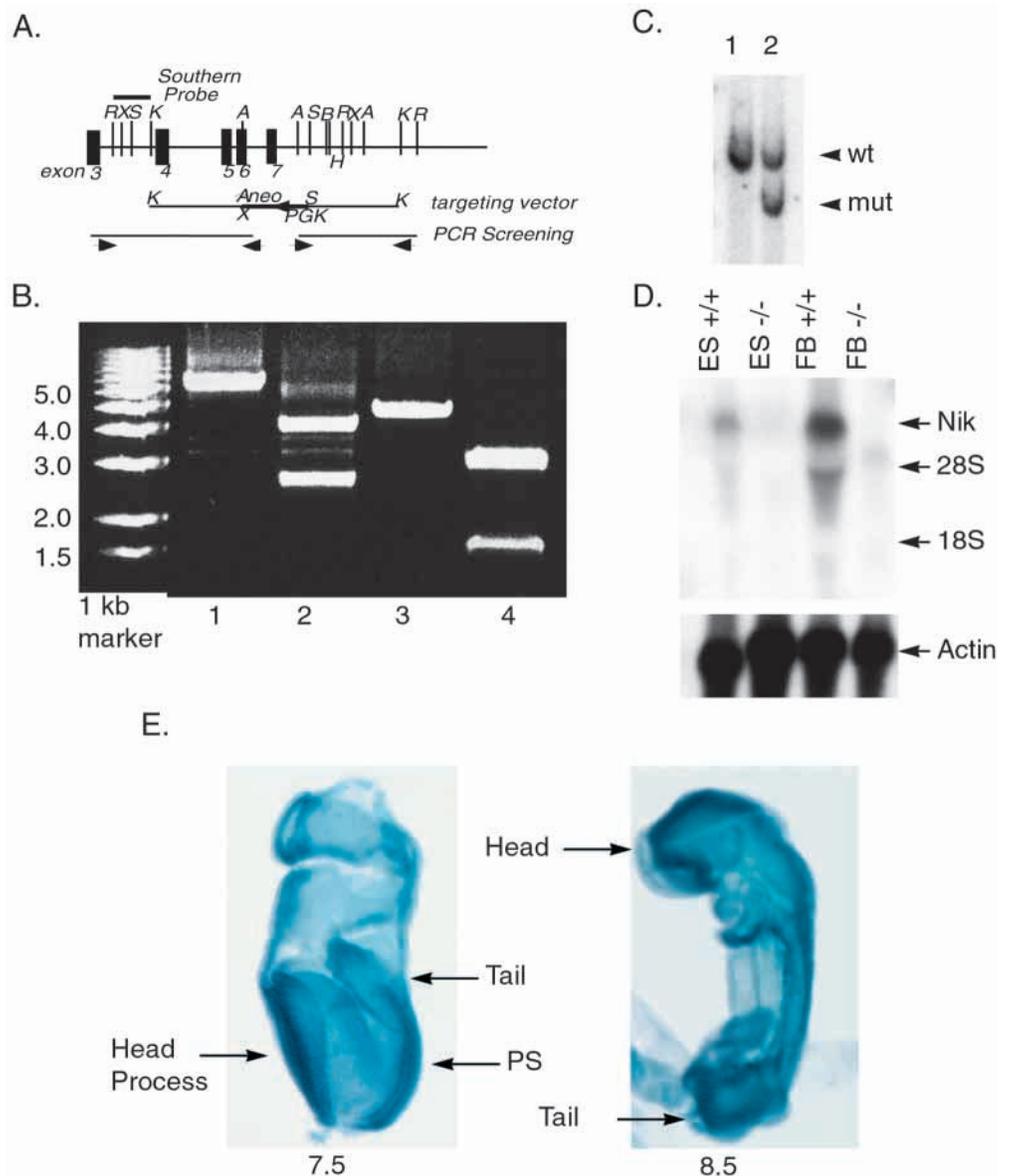
phenotype. *Nik*^{−/−} embryos appeared developmentally retarded and were smaller than control embryos (compare Fig. 2A and B). The most obvious defect in the *Nik* mutants was the absence of somites in most E8.5-9.0 *Nik*^{−/−} embryos, while comparably staged wild-type and heterozygous *Nik* littermates developed between 10 and 15 somites (compare Fig. 2C and E with D and F). While occasional *Nik* mutants (<10%) formed 1-2 somites anteriorly, no posterior somites were seen in any of the *Nik* mutants. In addition, *Nik* mutants failed to elongate posteriorly and a large mass of cells protruded from the region of the posterior primitive streak (PS) in most E8.5 *Nik* mutants (Fig. 2A,C). This led to a truncated body axis that connected a relatively normal anterior neural fold-like structure to a relatively normal allantois. These findings suggested that the major defect in *Nik* mutants is the failure to form normal mesodermal precursors that give rise to presomitic mesoderm as well as the mesoderm that contributes to the elongation of the body axis.

A defect in migration of mesodermal precursors away from

the PS could account for both the failure to form presomitic mesoderm and the accumulation of cells in the *Nik* mutants (Fig. 2). Alternatively, a defect in ingression of epiblasts into the streak could account for the *Nik* mutant phenotype. In order to distinguish between these two possibilities and to determine the origin of the cells stuck in the region of the PS in *Nik*^{−/−} embryos, expression of two T-box transcription factors, *Tbx6* and brachyury (*T*), was examined. Mesodermal tissue arises during gastrulation when epiblast cells move through the primitive streak forming a new layer of mesodermal cells located between the epiblasts and the outer visceral endoderm cells, beginning at E6.5 (Beddington, 1998; Beddington and Robertson, 1999). Previous experiments have indicated that induction of the T-box gene family of DNA binding transcription factors plays a central role in specifying the transition of epiblast to presomitic mesoderm (Yamaguchi et al., 1999). More recent data has shown that *T* gene expression is induced in epiblasts ingressing through the streak via a Wnt3A stimulated pathway and brachyury in turn induces

either directly or indirectly the expression of *Tbx6* (Yamaguchi et al., 1999). While *Tbx6* was expressed in cells adjacent to the PS in both control and *Nik*$^{-/-}$ embryos, it was also expressed in the large mass of cells that accumulated adjacent to the PS in E8.5 *Nik*$^{-/-}$ embryos (figure 3). In contrast, *T*, which is normally expressed in the PS, notochord and head process, and whose expression is normally turned off after cells leave the streak, was not expressed in the extra cells that accumulate in *Nik*$^{-/-}$ embryos. These findings indicate that the extra cells that accumulate in *Nik*$^{-/-}$ embryos have ingressed through the PS and have acquired a mesodermal fate. Since these extra cells in *Nik*$^{-/-}$ embryos express *Tbx6* but not *T*, they are most likely early presomitic mesoderm cells that fail to migrate to their appropriate paraxial position.

To confirm that *Nik* mutants have decreased presomitic mesoderm, E8.5 *Nik* mutants were stained for *mox1* (*meox1*) a homeobox gene whose expression is restricted to presomtic mesoderm and developing somites (Candia et al., 1992). Whole-mount in situ hybridization revealed that the *Mox1* transcript was markedly decreased in *Nik* mutants when compared to control embryos; *Mox1* expression was limited to the anterior paraxial region of the *Nik*$^{-/-}$ embryos in a more restricted area when compared to control embryos (Fig. 3). The extra cells that accumulate in the PS in *Nik* mutants do not express Mox1 and therefore are likely arrested as presomitic mesodermal cells. Previous studies have demonstrated that different signals are required for the generation of the first 7-9 somites up to the level of the proximal forelimb and for the remaining somites (Takada et al., 1994; Chapman and Papaioannou, 1998). For example, Wnt3a is required for the development of the more posterior somites, but is not required for the generation of the first 7-9 somites (Takada et al., 1994). Thus, our findings suggest that NIK is most important for generating presomitic mesoderm that develops into the more posterior somites. However, NIK likely plays other roles that are important for the organization of presomitic mesoderm into somites, because even when presomitic mesoderm is present, it is rarely found to organize into somites (Figs 2 and 3 and data not shown).

Mesodermal precursors other than presomitic mesoderm are present in *Nik*$^{-/-}$ embryos

Fate mapping studies have demonstrated that several different types of mesodermal cells arise from the PS and the specificity of these cells is determined by the position along the streak into which the epiblasts enter (Tam and Behringer, 1997). Epiblasts that migrate early through the posterior primitive streak are destined to become extraembryonic mesoderm, blood vessels, and cardiac mesoderm. Epiblast cells that migrate through the midstreak region are destined to

become lateral and intermediate mesoderm, while epiblasts migrating through the anterior PS are destined to become presomatic mesoderm and hindgut endoderm. The most anterior region of the streak is the node or organizer and epiblasts that migrate through the node give rise to the notochord and the fore and midgut endoderm.

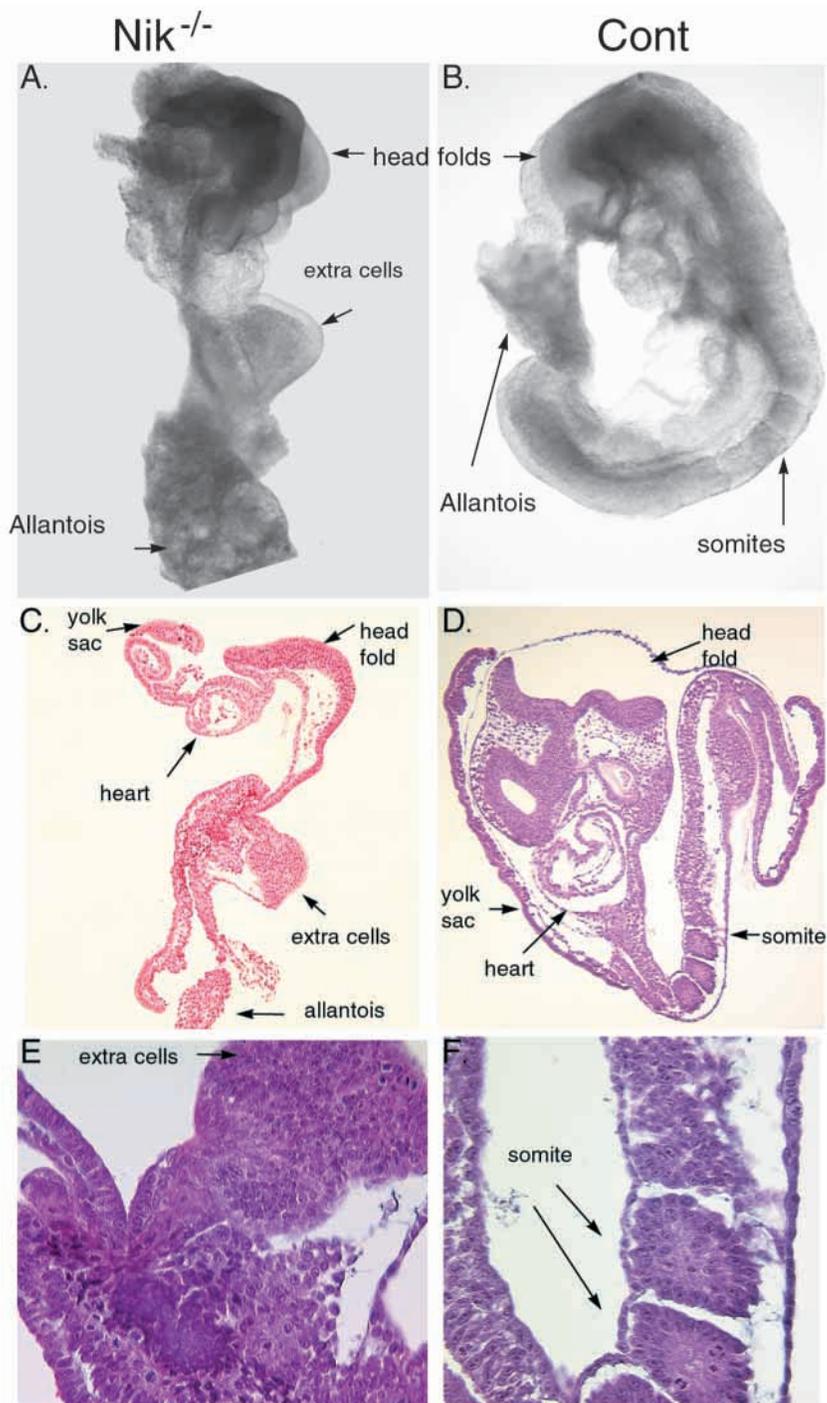To determine whether defects in mesodermal development

Fig. 2. Morphology of E8.5-9.0 control (B) and mutant embryos (A). Whole-mount sagittal section of E8.5-9.0 control (D,F) and mutant (C,E) embryos. E and F are a high magnifications of C and D. *Nik*$^{-/-}$ embryos lack somites and contain an extra mass of cells in the region of the PS.
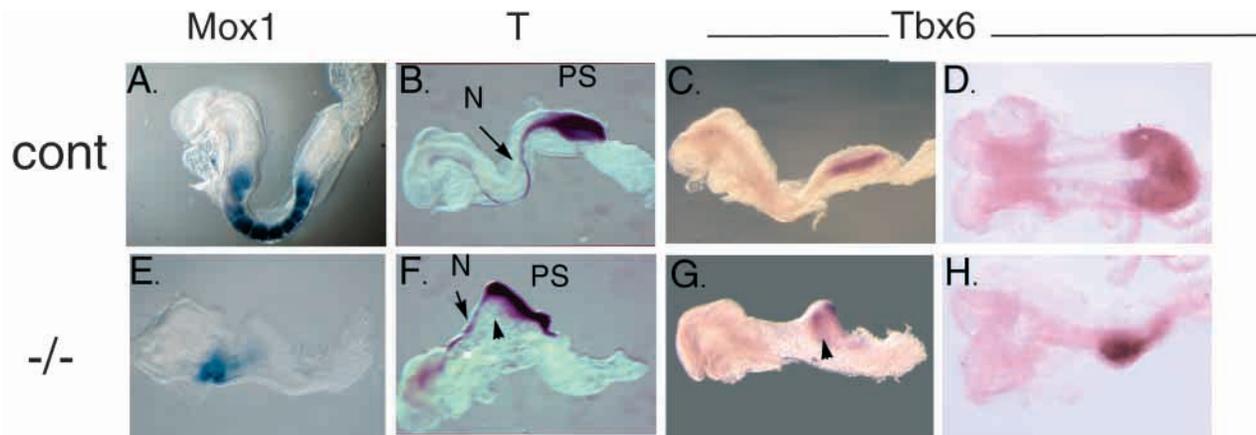
Fig. 3. Whole-mount in situ hybridization analysis of E8.5 *Nik*^{−/−} embryos for markers of paraxial mesoderm. E8.5 control (cont) or *Nik* homozygous mutant embryos (−/−) stained for *Mox1*, Brachyury (*T*) and *Tbx6* as indicated. All panels are lateral views except D and H which are dorsal views. N, notochord; PS, primitive streak. *mox1* staining cells are markedly decreased in the mutant and confined to the anterior domain of the embryo. The extra mass of cells that accumulate adjacent to the PS in the mutant embryos (marked with an arrowhead) do not stain for *T* or *mox1*, but do stain for *Tbx6*.

were confined to the presomitic mesoderm or whether development of other mesodermal compartments and endoderm were affected in the *Nik* mutants, *Nik*^{−/−} embryos were analyzed morphologically and for a number of different markers expressed in mesodermal tissues of specific origin. We found that *Nik*^{−/−} embryos formed extraembryonic mesodermal tissue such as the allantois, which eventually fuses with the chorion to form part of the placenta (see Fig. 2). In addition, *Nik* mutant embryos formed blood vessels. We used *Tie2-lacZ* expression as a marker to label endothelial cells (Schlaeger et al., 1997). Although the vasculature is disorganized in E9.5 *Nik* mutants when compared to wild-type embryos, endothelial cells are clearly visible in the yolk sac, head process and in the midline in E9.5 *Nik*^{−/−} embryos (Fig. 4). *Nik*^{−/−} embryos also contain a heart (Fig. 4). Cardiac mesoderm is formed and

organizes into a functional organ in the *Nik*^{−/−} embryo as is evident by a beating heart in E9.0 *Nik*^{−/−} embryos. Thus, these findings indicate that mesoderm that arises from the posterior and middle region of the PS is specified normally.

To determine whether structures derived from the anterior end of the streak, specifically the node and notochord are normal in *Nik* mutants, we examined the expression of *sonic hedgehog* (*Shh*). *Shh* has previously been shown to be expressed in the notochord, hindgut and the ventral midline of the brain (Echelard et al., 1993). In control embryos, *Shh* expression was visible throughout the entire anteroposterior axis (Fig. 4). In contrast, *Shh* expression was visible only in the notochord and head process in the NIK mutants (Fig. 4). Expression of *Shh* was not visible posteriorly in the NIK mutants in the region corresponding to the hindgut in wild-type

Fig. 4. Analysis of E8.5 and E9.5 *Nik*^{−/−} embryos for regional-specific markers of mesodermal differentiation. (A,B) Whole-mount staining for β-galactosidase, of embryos that are transgenic for *Tie2/lacZ* alone (A) or transgenic for *Tie2/lacZ* and homozygous mutant for *Nik* (B). Although the vasculature is disorganized in *Nik*^{−/−} embryos, β-galactosidase staining is clearly visible throughout the embryo. In addition, a heart is visible in *Nik* mutants indicating that mesoderm that gives rise to cardiac mesoderm forms normally in *Nik*^{−/−} embryos. Whole-mount staining of wild-type (C) or *Nik*^{−/−} embryos (D) for *sonic hedgehog* (*Shh*). Lateral views are shown in C and D. While *Nik*^{−/−} embryos have a notochord, they lack staining in the posterior part of embryos which corresponds to hindgut endoderm.
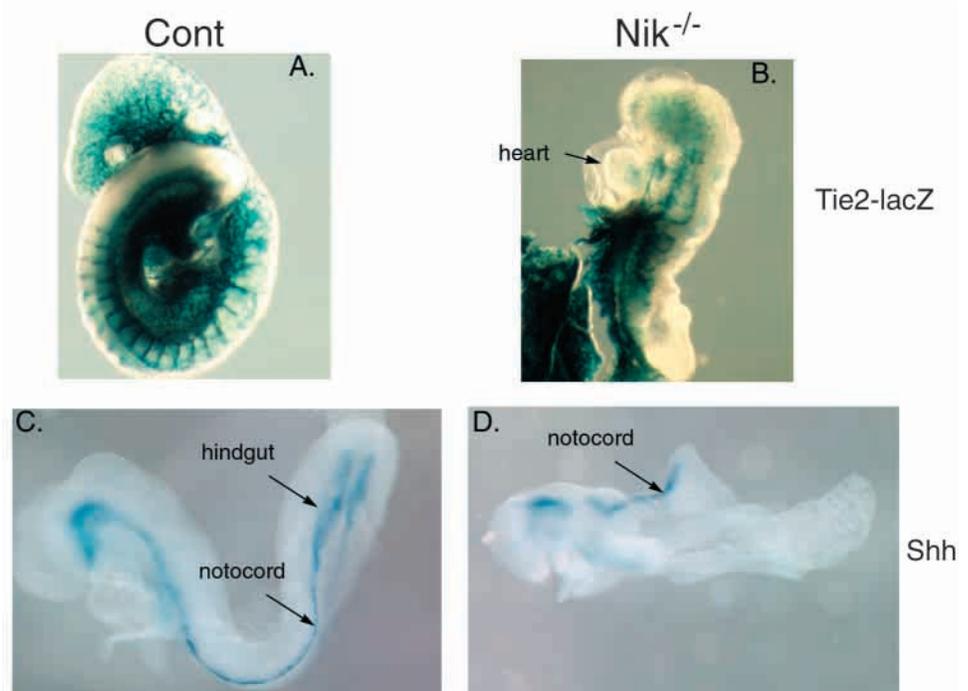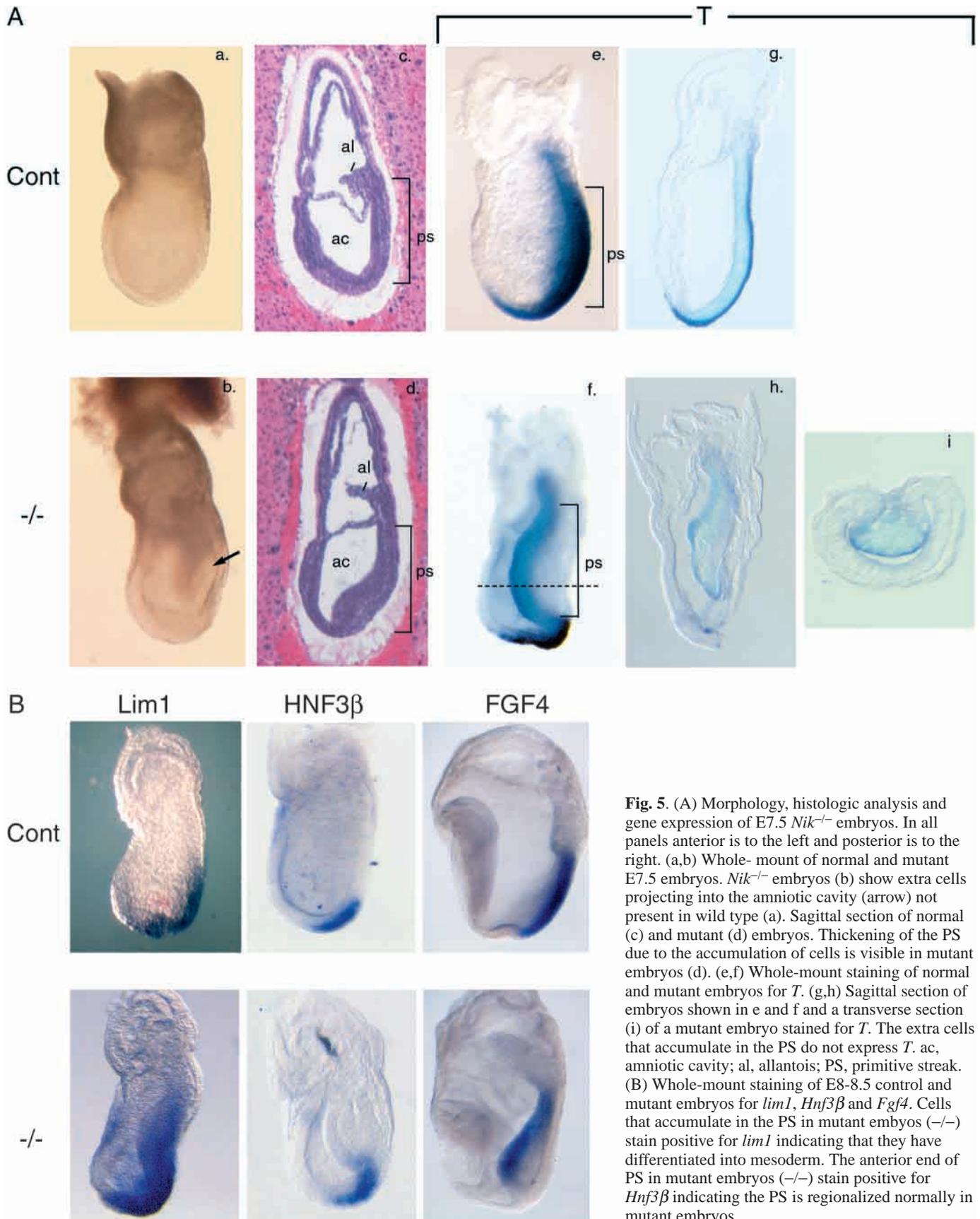
Fig. 5. (A) Morphology, histologic analysis and gene expression of E7.5 *Nik^−/−* embryos. In all panels anterior is to the left and posterior is to the right. (a,b) Whole- mount of normal and mutant E7.5 embryos. *Nik^−/−* embryos (b) show extra cells projecting into the amniotic cavity (arrow) not present in wild type (a). Sagittal section of normal (c) and mutant (d) embryos. Thickening of the PS due to the accumulation of cells is visible in mutant embryos (d). (e,f) Whole-mount staining of normal and mutant embryos for *T*. (g,h) Sagittal section of embryos shown in e and f and a transverse section (i) of a mutant embryo stained for *T*. The extra cells that accumulate in the PS do not express *T*. ac, amniotic cavity; al, allantois; PS, primitive streak. (B) Whole-mount staining of E8-8.5 control and mutant embryos for *lim1*, *Hnf3β* and *Fgf4*. Cells that accumulate in the PS in mutant embyos (−/−) stain positive for *lim1* indicating that they have differentiated into mesoderm. The anterior end of PS in mutant embryos (−/−) stain positive for *Hnf3β* indicating the PS is regionalized normally in mutant embryos.

embryos. In addition, in some mutants there was discontinuous staining in the region between the notochord and head process. These findings, when coupled with the staining for *T* shown in Fig. 3, suggest that axial mesoderm is formed normally in *Nik*⁻/⁻ embryos. The failure of *Shh* to stain gut endoderm suggests that precursor cells destined to form these structures are either not specified or are specified but fail to migrate to their proper location. It is intriguing that cells destined to form hindgut, but not mid and foregut endoderm, derive from common epiblast precursors that also give rise to presomitic mesoderm (Dufort et al., 1998). Thus, a defect in migration of a common meso/endoderm precursor could account for the decrease in both presomitic mesoderm and hindgut endoderm in *Nik*⁻/⁻ embryos.

Nik mutant embryos have a thickened anterior primitive streak

If failure of presomitic mesoderm to migrate away from the PS accounts for the defect in presomitic mesoderm and hindgut endoderm, thickening of the PS should be visible early in development. To evaluate the PS, midstreak E7-7.5 *Nik*⁻/⁻ embryos and control embryos were dissected and sectioned in their decidua. At this early time, *Nik*⁻/⁻ embryos could clearly be distinguished from wild-type embryos by thickening on their posterior side (compare Fig. 5A, a and b). In comparison to *Nik*⁺/⁺ and *Nik*⁺/⁻ embryos, *Nik*⁻/⁻ embryos contained an extra mass of cells on their posterior side that formed an indentation into the proamniotic cavity which in transverse sections were revealed as a thickening of the mid to anterior region of the PS (compare Fig. 5A, a and c with b and d).

To further examine the PS in *Nik* mutants, expression of several markers were evaluated by in situ hybridization. At E7.5, the *T* gene normally marks cells of the PS and axial mesoderm (Fig. 5A, e; Wilkinson et al., 1990). In *Nik*⁻/⁻ embryos, *T* is expressed in the bulge of cells adjacent to amniotic cavity along the proximodistal axis as well as in cells anterior to the PS. *T* is not expressed in the more posteriorly localized cells that accumulate in the PS in the *Nik*⁻/⁻ embryos (Fig. 5A f, h and i).

We next determined whether the cells in *Nik*⁻/⁻ embryos that accumulate in the PS and fail to stain for *T* express *lim1* (*Lhx1*). *lim1* is expressed at high levels in mesodermal cells migrating away from the PS (Barnes et al., 1994). Therefore, if the *T*-negative cells that accumulate in *Nik*⁻/⁻ embryos have undergone a transition to mesoderm they would be expected to stain for *lim1*. Consistent with this idea, we found that these cells do express *lim1* RNA (Fig. 5B). These findings, when taken with the results in Fig. 2, indicate that the extra cells that accumulate in *Nik*⁻/⁻ embryos have undergone an epiblast to mesoderm transition.

Nik mutants were also examined for *Hnf3β* (*Foxa2*) expression to determine whether the anterior half of the PS was correctly patterned, as pattering defects could account for the lack of presomitic mesoderm and hindgut endoderm in the *Nik* mutants; *Hnf3β* is normally expressed in cells at the anterior end of the PS (Ang et al., 1993). We found that *Hnf3β* is expressed in cells in the anterior half of the bulging PS in *Nik* mutant embryos indicating that defects in patterning of the PS do not account for the phenotype in *Nik*⁻/⁻ embryos (Fig. 5B).

Patterning of the anterior neuroectoderm is normal in the NIK mutants

To assess whether patterning of the anterior neuroectoderm is normal in *Nik* mutants, E8.5 control and *Nik*⁻/⁻ embryos were stained with *engrailed 1 (En1)*, *Krox20 (Egr2)*, *Otx2* and *Gbx2*. *En1,* normally expressed at the midbrain hindbrain boundary (Davis and Joyner, 1988) and, *Otx2*, normally expressed in the prospective forebrain and midbrain (Simeone et al., 1993), are expressed at relatively normal levels and in the correct distribution in *Nik*⁻/⁻ embryos (Fig. 6). In addition, *Gbx2,* which is expressed in the anterior hindbrain as well as distally through the PS to the posterior end of the embryo, and *Krox20* which is expressed in rhabdomeres 3 and 5 are expressed in a normal distribution in the *Nik*⁻/⁻ embryos (Fig. 6). These findings indicate that patterning of the anterior neuroectoderm is not perturbed in *Nik*⁻/⁻ embryos.

Chimera analysis with *Nik*⁻/⁻ ES cells

The above data suggest that the major abnormality in *Nik* mutant embryos is the failure of committed mesodermal cells to migrate away from the PS. In an attempt to directly demonstrate a defect in migration of *Nik*⁻/⁻ cells, and to confirm that the defect in cell migration is cell autonomous, we generated *Nik*⁻/⁻ ES cells. *Nik*⁻/⁻ ES cells were then used to aggregate ROSA26 *lacZ* mice. The ROSA *lacZ* transgene is ubiquitously expressed throughout early to mid gestational development and has been shown to be a good marker for distinguishing mutant and wild-type cells in chimeric embryos (Friedrich and Soriano, 1991). In these experiments, *Nik*⁻/⁻ ES cells lack β-galactosidase and do not stain while wild-type cells express β-galactosidase and stain blue. We obtained embryos with variable degrees of chimerism with *Nik*⁻/⁻ ES cells (Fig. 7). High degree chimerisms resulted in an embryonic phenotype that was similar to the NIK knockouts (Fig. 7A). However, analysis of embryos with lower amounts of chimerism (Fig. 7B) failed to demonstrate the accumulation of *Nik*⁻/⁻ ES cells in regions adjacent to the primitive streak (data not shown). *Nik*⁻/⁻ ES cells also contributed to hindgut (Fig. 7K,L). Thus, these findings indicate that migration of *Nik*⁻/⁻ ES cells away from the PS is normal in chimeric embryos.

We next evaluated the contribution of *Nik*⁻/⁻ ES cells to somites. Each somite begins as an epithelial sphere with a centrally arranged lumen of mesenchymal cells called a somitocoel (reviewed by Keynes and Stern, 1988; Tam and Trainor, 1994). In response to signals arising from surrounding structures the somitocoel eventually matures into three distinct compartments, which are, the sclerotome, myotome and dermatome. The sclerotome, which gives rise to the ribs and vertebrae, forms from the medial ventral half epithelium of the somitocoel that has reacquired a mesenchymal phenotype, as well as from the mesenchymal cells in the center of the somitocoel. The dorsolateral epithelium that remains forms a cap that is termed the dermomyotome. Cells of the dermomyotome ultimately give rise to the dermis of the dorsal skin and to myotome cells which form the hypaxial and epaxial muscles of the trunk and limbs.

We found that mesoderm arising from *Nik*⁻/⁻ ES cells migrated to the appropriate position in the chimeric embryos (Fig. 7). *Nik*⁻/⁻ ES cells contributed equally well as wild-type ES cell to presomitic mesoderm and hindgut endoderm (Fig. 7K,L and data not shown). However, in contrast to the wild-

type cells, that were incorporated into the dermomyotome, *Nik*⁻/⁻ ES cells were excluded from the segmented dermomyotome in all embryos examined (7/7) (Fig. 7C-J). The inability of *Nik*⁻/⁻ ES cells to contribute to the dermomyotome layer of the somite is likely specific because *Nik*⁻/⁻ ES cells contributed to and competed equally well with wild-type cells in all other tissues examined including the neural tube and heart (Fig. 7I,L and data not shown).

To evaluate somites at different stages of differentiation in chimeric embryos, additional sections from control and chimeric embryos were stained for β-galactosidase. Somites develop over time in a rostral to caudal progression, and thereby the more rostrally localized somites have the opportunity to undergo further differentiation towards a mature somite compared to the newly formed somites that are located caudally. Examination of somites at the early somitocoel stage of somite development demonstrated that *Nik*⁻/⁻ ES were virtually completely excluded from the surrounding epithelium (Fig. 7H). In contrast, the centrally located mesenchymal cells were composed almost entirely of *Nik*⁻/⁻ ES cells (Fig. 7H). We hypothesize that the phenotype of the mature somite in which *Nik*⁻/⁻ ES are excluded from the epithelial cap of the dermomyotome arises as the wild-type ventromedial epithelium reacquires a mesenchymal phenotype. At present, we do not know whether the centrally localized *Nik*⁻/⁻ ES are trapped passively by the wild-type cells or are actively recruited to this compartment and are able to go on to form more mature structures that arise from the sclerotome. Nevertheless, these findings indicate that NIK plays two roles in generating somites: (1) NIK has a cell nonautomonous function to stimulate migration of presomitic mesoderm away from the PS; and (2) NIK is cell-autonomously required for differentiation of the dermomyotome of the somite.

Expression of FGF4 in E8.0 *Nik* mutants

The accumulation of mesodermal cells in the PS in *Nik* mutants resembles in some respects knockout studies of *fibroblast growth factor (Fgf) 8* and *Fgfr1* (*fibroblast growth factor receptor 1*; Deng et al., 1994; Sun et al., 1999; Yamaguchi et al., 1994). In *Fgf8*⁻/⁻ embryos, epiblast cells pass through the PS and undergo an epithelial to mesenchyme transition, but essentially no mesodermal precursors move away from the PS, leading to almost complete absence of mesodermally and endodermally derived embryonic tissue (Sun et al., 1999). The defect in migration of *Fgf8*⁻/⁻ ES cells from the PS is, like NIK, cell nonautonomous (Sun et al., 1999). Thus, these data are consistent with the possibility that NIK mediates some of FGF8's functions in the PS to stimulate production of a secreted molecule(s) required for cell migration. FGF4 has been hypothesized to be one of the molecules that functions downstream of FGF8 and whose production in the PS is required for the normal migration of mesodermal cells away from the PS (Sun et al., 1999). Therefore, to determine whether NIK may impinge on a common pathway with FGF8, we determined the expression of *Fgf4* in *Nik*⁻/⁻ embryos by in situ hybridization. We found that expression of *Fgf4* in the PS is normal in E8.5 *Nik*⁻/⁻ embryos (Fig. 5B). These findings are consistent with either NIK and FGF8 functioning in independent pathways or NIK functioning downstream of FGF8 and FGF4.

DISCUSSION

Requirement for NIK in early embryonic development

Homologs of the mammalian Ste20 kinase NIK have previously been shown to be essential for development in both *Drosophila* and *C. elegans*. In view of the large number of Ste20 kinases in mammalian cells, it was possible that NIK would not be essential for mammalian development because of redundant function with other Ste20 kinases. However, despite the large number of Ste20 kinases in mammalian cells, we found that NIK is indeed essential for development in mammalian cells. *Nik*⁻/⁻ mice die postgastrulation between E9.5 and E10.5. The most striking phenotype in mice containing a targeted disruption of NIK is the failure of mesodermal and endodermal cells that arise from the anterior end of the PS to migrate to their correct location. As a result *Nik*⁻/⁻ embryos fail to develop somites or a hindgut and contain an extra mass of cells that accumulate in the region of the PS. These extra cells are most likely to be committed mesoderm cells that fail to migrate away from the PS, since they stain positive for the mesodermal markers *lim1* and *Tbx6*. *Nik*⁻/⁻ mice are also developmentally delayed and truncated posteriorly, suggesting that NIK also regulates the mesodermal migration that contributes to the elongation of the body axis. While we cannot exclude the possibility that decreased proliferation and/or survival of mesodermal precursors accounts for the growth retardation and posterior truncation of *Nik*⁻/⁻ embryos, the finding that *Nik*⁻/⁻ ES cells contribute equally to wild-type cells in chimeric embryos suggests that NIK does not regulate either cell proliferation or survival.

While paraxial mesoderm and hindgut endoderm are affected in *Nik*⁻/⁻ embryos, defects were not found in several other mesodermal and endodermal lineages. Extraembryonic mesoderm including the allantois, yolk sac and blood vessels are present in *Nik*⁻/⁻ embryos. In addition, *Nik*⁻/⁻ embryos form a heart and axial mesoderm. Fate mapping studies have indicated that the specific fate of mesodermal cells correlates with the level along the proximodistal (PD) border in which epiblasts migrate through the PS (Tam and Behringer, 1997; Beddington, 1998; Beddington and Robertson, 1999). The finding that both presomitic mesoderm and hindgut endoderm arise from the region of the PS just posterior to the node suggests that NIK plays a critical and specific role in regulating the migration of cells that arise from this position of the PS. Evidence for regional variation in the signals required for migration of cells leaving the PS has recently been provided by a study of *Fgf8* knockout mice (Sun et al., 1999). Although migration of mesodermal precursors is more severely affected in Fgf8 knockouts than in *Nik* knockouts, leading to an almost complete lack of development of embryonic tissues, migration of mesoderm arising from more proximal regions of the PS that gives rise to extraembryonic mesoderm and blood is not affected in such *Fgf8* knockouts.

Chimeric analysis of mice using *Nik*⁻/⁻ ES cells demonstrated that the inability of *Nik*⁻/⁻ cells to migrate away from the PS is not due to loss of NIK in these mesodermal precursors. We found that E9.5 chimeric embryos with less than 50% contribution of *Nik*⁻/⁻ ES cells were phenotypically normal and accumulation of cells adjacent to the PS was not found. In addition, *Nik*⁻/⁻ cells contribute to paraxial mesoderm in chimeric embryos and the contribution of *Nik*⁻/⁻ cells to

paraxial mesoderm is proportional to their contribution to the rest of the embryo. These findings indicate that NIK functions cell nonautonomously to regulate the production of a factor that stimulates the migration of mesodermal precursors destined to from paraxial mesoderm away form the PS. The effector cell on which NIK is acting is currently not known; in situ analysis has demonstrated that NIK is ubiquitously expressed in most tissues including the primitive streak. In addition to NIK's cell nonautonomous effect to stimulate migration of paraxial mesodermal precursors away from the PS, NIK also has a cell autonomous effect to stimulate epithelialization of somites. We found that in contrast to the wild-type cells, $Nik^{-/-}$ ES cells were excluded from the surrounding epithelium compartment of the somitocoel as well as the segmented dermomyotome.

Phenotype in the *Nik* mutant embryos is not due to defective activation of JNK

While *Nik* and its *Drosophila* homolog *msn* have been linked both genetically and biochemically to the activation of the JNK MAP kinase pathway, the phenotype in *Nik* nullizygous embryos is unlikely to be due to defective activation of JNK (Su et al., 1997; Su et al., 1998). The JNK family consists of at least 10 isoforms of alternatively spliced genes arising from alternative splicing of three JNK genes. While *JNK1* (*Mapk8*) and *JNK2* (*Mapk9*) are ubiquitously expressed, *JNK3* (*Mapk10*) has been found to be mainly expressed in the CNS (Martin et al., 1996). While mice lacking individual members of *JNK1, JNK2* and *JNK3* all survive normally, mice deficient in both *JNK1* and *JNK2* die embryonically at day 11.5 (Kuan et al., 1999). The most obvious phenotype in *JNK1, JNK2* double deficient embryos is hindbrain exencephaly as a result of reduced apoptosis in the lateral edges of the hindbrain (Kuan et al., 1999). However, the overall morphology of the *JNK1, JNK2* double mutants is similar to wild-type embryos and somite formation in the *JNK1, JNK2* double mutants is normal. Thus, these findings, coupled with the finding that the only other JNK gene, *JNK3*, is restricted to the CNS, would suggest that the defects observed in the *Nik* homozygous mutants are unrelated to JNK activation. We cannot, however, exclude the possibility that NIK also functions later in development to activate JNK because the $Nik^{-/-}$ mice die before the *JNK1, JNK2* double knockouts.

The ability of NIK to activate JNK-independent pathways and to function during gastrulation is also consistent with genetic experiments in *Drosophila.* In evaluating *msn* mutant flies rescued with a kinase defective Msn, we observed that many *msn* mutants had ventral cuticular abnormalities, suggesting a defect in gastrulation (Su et al., 2000). The role of *msn* in this phenotype is likely independent of JNK activation because ventral defects are not observed in embryos lacking both maternal and zygotic *Drosophila* (D)JNK (*bsk*) or the *Drosophila* JNK kinase encoded by *hep* (Glise, 1995; Riesgo-Escovar, 1996). Given the conservation between NIK and Msn, it is intriguing to speculate that the

defects in cell migration in $Nik^{-/-}$ mice, and the ventral defects in *msn* mutant flies, are due to the failure of both kinases to activate similar signaling pathways. The nature of the signaling pathways regulated by either NIK or Msn that regulate either of these processes are currently not known.

Signaling pathways in which NIK functions in development

In addition to determining NIK's role in development, we also hoped to identify, in these genetic studies, the upstream signals that regulate NIK in mammalian cells. We initially identified NIK on the basis of its ability to bind the SH3 domains of Nck (Su et al., 1997). Thus, we hypothesized that NIK may function downstream of a tyrosine kinase during development; in response to activation of a tyrosine kinase, NIK bound to the SH3 domains of NCK may be recruited to phosphotyrosine-containing proteins via the SH2 domain of NCK. In this regard, NCK has been shown to be recruited to the FGFR signaling pathway in experiments in cells (Gupta and Mayer, 1998; Liu et al., 1999; Rockow et al., 1996), and mice containing a targeted disruption of *Fgf8* or *Fgfr1* resemble the *Nik* mutant phenotype reported here in some aspects (Sun et al., 1999;
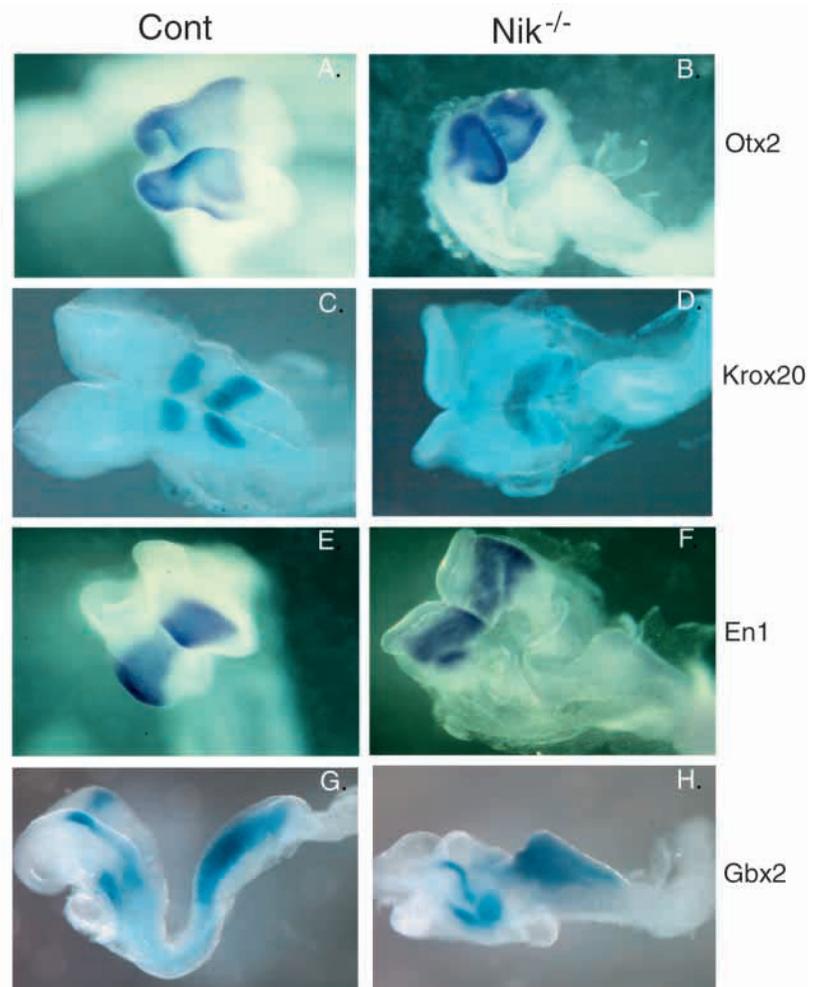

Fig. 6. Patterning of the anterior neuroectoderm. Whole-mount staining of wild-type (cont) and $Nik^{-/-}$ embryos for *Otx2*, *En1, Krox20* and *Gbx2* as indicated. All pictures are dorsal views with the head to the left and the tail to the right.

Yamaguchi et al., 1994). Mice nullizygous for *Fgf8* or *Fgfr1* are similar to *Nik* nullizygous mice in that they both have a thickened PS due to the failure of mesodermal cells to migrate away from the PS (Deng et al., 1994; Sun et al., 1999; Yamaguchi et al., 1994). With respect to *Fgf8* and *Fgfr1* knockouts, the mice nullizygous for *Nik* more closely resemble less severely affected mice nullizygous for *Fgf8*. The cells that accumulate in the PS in mice nullizygous for both *Fgf8* and *Nik* have undergone an epithelial-to-mesenchymal (E-M) transition (Sun et al., 1999). In addition, chimeric analysis of *Fgf8⁻/⁻* ES cells is similar to chimeric analysis of *Nik⁻/⁻* ES cells in that the defect in migration of *Fgf8⁻/⁻* mesodermal cells away from the PS is cell nonautonomous; *Fgf8⁻/⁻* ES cells contributed to all tissues in chimeric embryos (Sun et al., 1999). However, while these findings are consistent with the possibility that the phenotype in *Nik⁻/⁻* embryos is due to inhibition of some aspects of Fgf signaling, differences exist between the *Nik* and the *Fgf8* knockouts that suggest that the phenotype of the *Nik⁻/⁻* embryos is not due to loss of FGF signaling. Decreased expression of *Fgf4* and *Tbx6* in the PS in *Fgf8* knockouts has been proposed to be responsible for the mesodermal defect in mice nullizygous for *Fgf8* (Sun et al., 1999). The finding that *Nik⁻/⁻* embryos express both *Fgf4* and *Tbx6* in the PS indicates that NIK does not mediate the induction of either of these genes by Fgf8. The large number of Fgfs and their receptors, as well as the importance of FGFs in mediating numerous

processes during development, may complicate the comparison between phenotypes of mice nullizygous for a single FGF ligand and/or receptor with mice nullizygous for a signaling molecule functioning downstream of these receptors. As a result, genetic analysis of *Nik* mutant mice and *Fgf* double mutants as well as analysis of *Fgf* responses in *Nik⁻/⁻* cell lines will be required to determine whether NIK ultimately regulates signals downstream of FGFs and their receptors.

The *Nik* knockout phenotype also resembles some aspects of phenotypes identified during knockout studies of components of the fibronectin (FN) signaling pathway. Analysis of embryos mutant for the extracellular matrix protein FN, integrin α5 which is a component of the fibronectin receptor, and Focal adhesion kinase (FAK), which
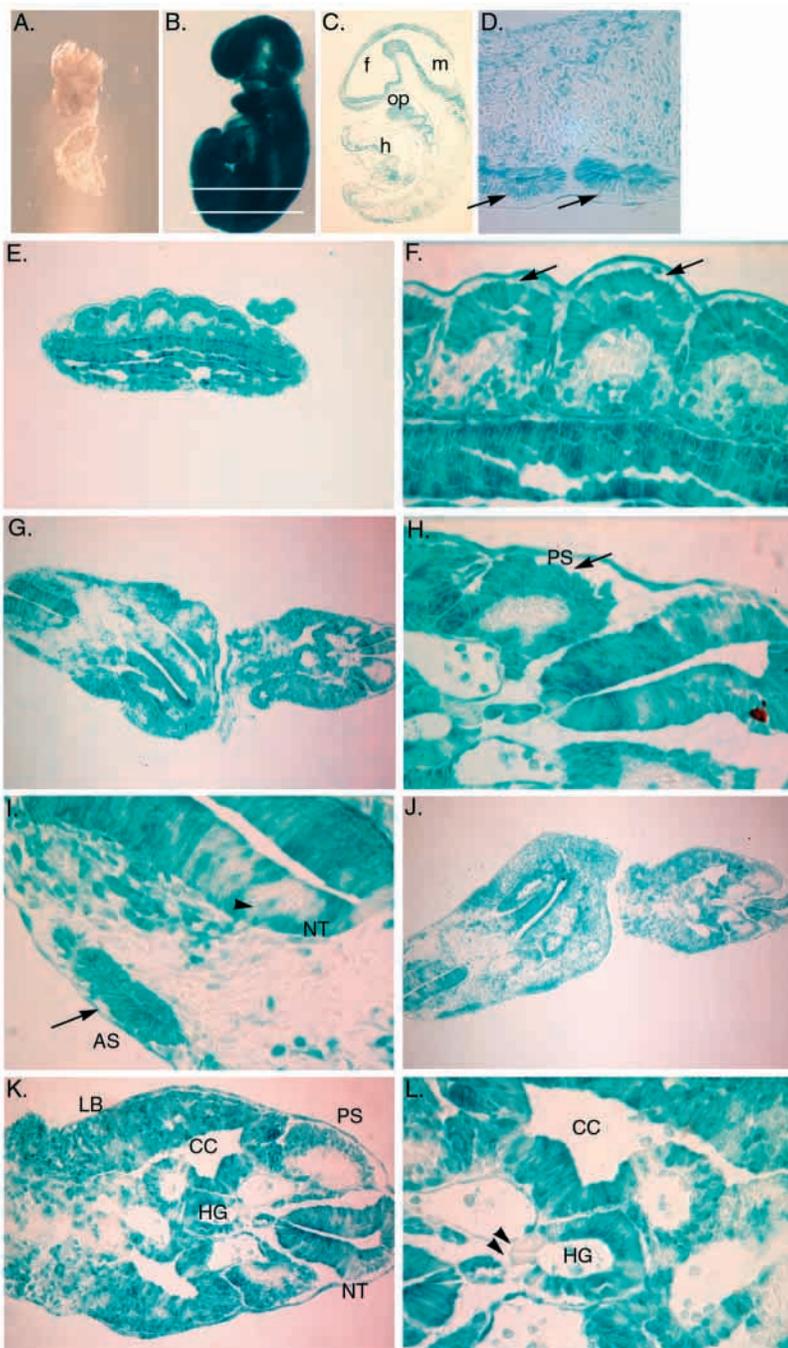

Fig. 7. Chimeric analysis of *Nik⁻/⁻* ES cells. (A,B) Whole-mount staining of E9.5 chimeric embryos for β-galactosidase. Chimeric embryos with a range of contribution of *Nik⁻/⁻* ES cells were obtained. Embryos with high contribution from *Nik⁻/⁻* ES cells (A) displayed a similar phenotype to *Nik* mutant embryos. Embryos with a lower contribution from *Nik⁻/⁻* ES cells (B as an example) were also sectioned sagitally (C,D) or transversely (E-J). E (100× magnification) and F (400× magnification) correspond to the lower transverse section shown in B while G-I correspond to the upper transverse section shown in B. *Nik⁻/⁻* ES cells which do not stain because they do not express β-galactosidase are excluded from the segmented dermomyotome (marked by an arrow) in mature somites (D-I). I is a higher magnification (400×) of the more mature anterior somite shown in G while H is a higher magnification (400×) of a posterior somites at an early somitocoel stage of development. Examination of somites at the early somitocoel stage of somite development demonstrated that *Nik⁻/⁻* ES were virtually completely excluded from the surrounding epithelium whereas the centrally located mesenchymal cells were composed almost entirely of *Nik⁻/⁻* ES cells (H). The ability of *Nik⁻/⁻* ES to contribute to hindgut endoderm is shown in J-L. K (200×) and L (400×) are higher magnifications of J showing that *Nik⁻/⁻* ES contribute to hindgut endoderm (HG) which is marked by 2 arrowheads. I shows that *Nik⁻/⁻* ES contribute to other tissues such as the neural tube (NT) which is marked by an arrowhead. f, forebrain; m, midbrain; op, oropharynx; h, heart; LB, limb bud; CC, coelomic cavity; AS, anterior somite; PS, posterior somite; and LB, limb bud.

is a cytosolic tyrosine kinase that mediates downstream signaling from the FN receptor, all have defects in mesoderm and lack somites (Furuta et al., 1995; Georges-Labouesse et al., 1996; Goh et al., 1997). However, the lack of somites in these mutants is primarily due to the failure of condensation of presomitic mesoderm into somites, rather than to the migration of mesodermal precursors cells away from the PS (Georges-Labouesse et al., 1996; Goh et al., 1997). Both FN and integrin α5 knockouts express the presomitic markers *notch1* and *mox1* in a normal pattern and do not have a thickened PS. It is tempting to speculate that the cell autonomous defect in differentiation of the dermomyotome of $Nik^{-/-}$ ES cell in chimeric embryos may reflect defects in signaling downstream of the FN receptor. In this regard, the SH2 domain of NCK has been shown to bind tyrosine phosphorylated p130Cas, a substrate for FAK, in FN-stimulated cells (Schlaepfer et al., 1997). The importance of p130Cas as a downstream target of FAK is supported by the finding that the defect in FN-stimulated assembly of actin filaments into stress fibers and migration of $FAK^{-/-}$ fibroblasts is rescued by ectopic expression of wild-type FAK, but not by expression of a mutant FAK that is unable to bind p130Cas (Sieg et al., 1999). We found that $Nik^{-/-}$ fibroblasts also exhibit defects in FN-stimulated assembly of actin filaments into stress fibers that resembles $FAK^{-/-}$ fibroblasts (data not shown). Thus, these findings raise the possibility that recruitment of a NCK/NIK complex to tyrosine phosphorylated p130Cas mediates one of the signals that is required for segmentation of presomitic mesoderm into somites.

Genetic experiments in flies have also indicated that Msn functions downstream of the Frizzled (Fz) receptor. *msn* mutants show a defect in planar polarity in both the wing and eyes due to the failure of Dsh, a downstream target of Fz, to activate JNK (Mlodzik, 1999; Paricio et al., 1999). The Fz protein in *Drosophila* functions as a receptor for Wingless (Wg), the *Drosophila* homolog of mammalian Wnts (Cadigan and Nusse, 1997). Interestingly, mice nullizygous for *Wnt3a* also lack caudal somites and are truncated posteriorly (Takada et al., 1994). However, NIK is not required for the activity of this *Wnt3a* signaling pathway. In *Wnt3a* mutants, unlike *Nik* mutants, epiblasts fail to undergo an E-M transition and form ectopic neural tubes rather than somites (Yoshikawa et al., 1997). *Wnt3a* induces the E-M transition by stimulating *T* gene expression in epiblasts ingressing through the PS via the activation of a signaling pathway that requires a transcriptional complex composed of β-catenin and a member of the Tcf family (Galceran et al., 1999; Yamaguchi et al., 1999). Brachyury in turn induces, either directly or indirectly, the expression of *Tbx6*, a T-box gene, which plays a critical role in specifying presomitic mesoderm (Chapman and Papaioannou, 1998; Yamaguchi et al., 1999) Experiments in *Drosophila* and in tissue culture cells have indicated that Dsh couples Fz receptors to two distinct signaling pathways which include the β-catenin/Tcf pathway and a second pathway that utilizes *msn* to activate the JNK MAP kinase pathway (Boutros et al., 1998; Li et al., 1999). While the biological relevance of the β-catenin/Tcf pathway in Wnt signaling and somite development in mammalian cells is now apparent, future studies will likely uncover critical roles for NIK and JNK in other mammalian Wnt signaling pathways.

Conclusion

Little is known about the specific roles played by members of the GCK Ste20 kinase family in mammals. The difficulty in studying these kinases has been augmented by the large number of kinases in this family coupled with the lack of information about the specific biological functions played by individual members of this group. Most studies to date have focused on the regulation of the JNK MAP kinase pathway by members of this family of kinases. However, studies in *Drosophila* as well as studies reported here demonstrate that the repertoire of signaling pathways regulated by GCK family of kinases needs to be expanded beyond activation of the JNK MAP kinase pathway. The difficulty in determining the function of Ste20 kinases in cell culture and the signaling pathways that they regulate reinforces the importance of identifying genetic systems in which to study individual members of this kinase family. In this regard, the study of *msn* in *Drosophila* and *Mig-15* in *C. elegans* has been extremely fruitful in clarifying and expanding our knowledge of Ste20 kinases in mammalian cells. The finding that NIK is critical for normal development demonstrates that redundancy among the many Ste20 kinases in mammals may be limited, and therefore that knockout studies of other Ste20 kinases are likely to yield important insights into the function of this interesting but complex family of kinases.

REFERENCES

Ang, S. L., Wierda, A., Wong, D., Stevens, K. A., Cascio, S., Rossant, J. and Zaret, K. S. (1993). The formation and maintenance of the definitive endoderm lineage in the mouse: involvement of HNF3/forkhead proteins. *Development* **119,** 1301-1315.

Barnes, J. D., Crosby, J. L., Jones, C. M., Wright, C. V. and Hogan, B. L. (1994). Embryonic expression of Lim-1, the mouse homolog of Xenopus Xlim-1, suggests a role in lateral mesoderm differentiation and neurogenesis. *Dev. Biol.* **161,** 168-178.

Becker, E., Huynh-Do, U., Holland, S., Pawson, T., Daniel, T. O. and Skolnik, E. Y. (2000). Nck-interacting Ste20 kinase couples Eph receptors to c-Jun N-terminal kinase and integrin activation. *Mol. Cell Biol.* **20,** 1537-1545.

Beddington, R. (1998). Cripto-analysis of embryonic codes [news; comment]. *Nature* **395,** 641-643.

Beddington, R. S. and Robertson, E. J. (1999). Axis development and early asymmetry in mammals. *Cell* **96,** 195-209.

Bouillet, P., Chazaud, C., Oulad-Abdelghani, M., Dolle, P. and Chambon, P. (1995). Sequence and expression pattern of the Stra7 (Gbx-2) homeobox-containing gene induced by retinoic acid in P19 embryonal carcinoma cells. *Dev. Dyn.* **204,** 372-382.

Boutros, M., Paricio, N., Strutt, D. I. and Mlodzik, M. (1998). Dishevelled activates JNK and discriminates between JNK pathways in planar polarity and wingless signaling. *Cell* **94,** 109-118.

Burbelo, P. D., Drechsel, D. and Hall, A. (1995). A Conserved Binding Motif Defines Numerous Candidate Target Proteins for Both Cdc42 and Rac GTPases,. *J. Biol. Chem.* **270,** 29072-29074.

Cadigan, K. M. and Nusse, R. (1997). Wnt signaling: a common theme in animal development. *Genes Dev.* **11,** 3286-3305.

Candia, A. F., Hu, J., Crosby, J., Lalley, P. A., Noden, D., Nadeau, J. H. and Wright, C. V. (1992). Mox-1 and Mox-2 define a novel homeobox gene subfamily and are differentially expressed during early mesodermal patterning in mouse embryos. *Development* **116,** 1123-1136.

Chapman, D. L., Agulnik, I., Hancock, S., Silver, L. M. and Papaioannou, V. E. (1996). Tbx6, a mouse T-Box gene implicated in paraxial mesoderm formation at gastrulation. *Dev. Biol.* **180,** 534-542.

Chapman, D. L. and Papaioannou, V. E. (1998). Three neural tubes in mouse embryos with mutations in the T-box gene Tbx6. *Nature* **391,** 695-697.

Creasy, C. L. and Chernoff, J. (1995a). Cloning and characterization of a member of the MST subfamily of Ste20- like kinases. *Gene* **167,** 303-306.

Creasy, C. L. and Chernoff, J. (1995b). Cloning and Characterization of Human Protein Kinase with Homology to Ste20. *J. Biol. Chem.* **270,** 21695-21700.

Davis, C. A. and Joyner, A. L. (1988). Expression patterns of the homeo box-containing genes En-1 and En-2 and the proto-oncogene int-1 diverge during mouse development. *Genes Dev.* **2,** 1736-1744.

Deng, C. X., Wynshaw-Boris, A., Shen, M. M., Daugherty, C., Ornitz, D. M. and Leder, P. (1994). Murine FGFR-1 is required for early postimplantation growth and axial organization. *Genes Dev.* **8,** 3045-3057.

Diener, K., Wang, X. S., Chen, C., Meyer, C. F., Keesler, G., Zukowski, M., Tan, T. H. and Yao, Z. (1997). Activation of the c-Jun N-terminal kinase pathway by a novel protein kinase related to human germinal center kinase. *Proc. Natl. Acad. Sci. USA* **94,** 9687-9692.

Dufort, D., Schwartz, L., Harpal, K. and Rossant, J. (1998). The transcription factor HNF3β is required in visceral endoderm for normal primitive streak morphogenesis. *Development* **125,** 3015-3025.

Echelard, Y., Epstein, D. J., St-Jacques, B., Shen, L., Mohler, J., McMahon, J. A. and McMahon, A. P. (1993). Sonic hedgehog, a member of a family of putative signaling molecules, is implicated in the regulation of CNS polarity. *Cell* **75,** 1417-1430.

Friedrich, G. and Soriano, P. (1991). Promoter traps in embryonic stem cells: a genetic screen to identify and mutate developmental genes in mice. *Genes Dev.* **5,** 1513-1523.

Furuta, Y., Ilic, D., Kanazawa, S., Takeda, N., Yamamoto, T. and Aizawa, S. (1995). Mesodermal defect in late phase of gastrulation by a targeted mutation of focal adhesion kinase, FAK. *Oncogene* **11,** 1989-1995.

Galceran, J., Farinas, I., Depew, M. J., Clevers, H. and Grosschedl, R. (1999). Wnt3a–/– like phenotype and limb deficiency in Lef1(–/–)Tcf1(–/–) mice. *Genes Dev.* **13,** 709-717.

Garrity, P. A., Rao, Y., Salecker, I., McGlade, J., Pawson, T. and Zipursky, L. (1996). Drosophila photoreceptor axon guidance and targeting requires the dreadlocks SH2/SH3 adapter protein. *Cell* **85,** 639-650.

Georges-Labouesse, E. N., George, E. L., Rayburn, H. and Hynes, R. O. (1996). Mesodermal development in mouse embryos mutant for fibronectin. *Dev. Dyn.* **207,** 145-156.

Glise, B., Bourbon, H., Noselli, S. (1995). Hemipterous encodes a novel Drosophila MAP kinase kinase required for epithelial cell sheet movement. *Cell* **83,** 451-461.

Glise, B. and Noselli, S. (1997). Coupling of Jun amino-terminal kinase and Decapentaplegic signaling pathways in Drosophila morphogenesis. *Genes Dev.* **11,** 1738-1747.

Goh, K. L., Yang, J. T. and Hynes, R. O. (1997). Mesodermal defects and cranial neural crest apoptosis in alpha5 integrin-null embryos. *Development* **124,** 4309-4319.

Gupta, R. W. and Mayer, B. J. (1998). Dominant-negative mutants of the SH2/SH3 adapters Nck and Grb2 inhibit MAP kinase activation and mesoderm-specific gene induction by eFGF in Xenopus. *Oncogene* **17,** 2155-2165.

Herrmann, B. G. (1991). Expression pattern of the Brachyury gene in whole-mount TWis/TWis mutant embryos. *Development* **113,** 913-917.

Hing, H., Xiao, J., Harden, N., Lim, L. and Zipursky, S. L. (1999). Pak functions downstream of Dock to regulate photoreceptor axon guidance in Drosophila. *Cell* **97,** 853-63.

Hou, X. S., Goldstein, E. S. and Perrimon, N. (1997). Drosophila Jun relays the Jun amino-terminal kinase signal transduction pathway to the Decapentaplegic signal transduction pathway in regulating epithelial cell sheet movement. *Genes Dev.* **11,** 1728-1737.

Hu, M. C., Qiu, W. R., Wang, X. R., Meyer, C. F. and Tan, T.-H. (1996). Human HPK1, a novel hematopoietic progenitor kinase that activates the JNK/SAPK kinase cascade. *Genes Dev.* **10,** 2251-2264.

Joyner, A. (1993). *Gene Targeting – A Practical Approach.* IRL Press, Oxford, UK.

Keynes, R. J. and Stern, C. D. (1988). Mechanisms of vertebrate segmentation. *Development* **103,** 413-429.

Kockel, L., Zeitlinger, J., Staszewski, L. M., Mlodzik, M., Bohmann, D. (1997). Jun in Drosophila development: redundant and nonredundant functions and regulation by two MAPK signal transduction pathways. *Genes Dev.***11,** 1748.

Kuan, C. Y., Yang, D. D., Samanta Roy, D. R., Davis, R. J., Rakic, P. and Flavell, R. A. (1999). The Jnk1 and Jnk2 protein kinases are required for regional specific apoptosis during early brain development. *Neuron* **22,** 667-676.

Kuramochi, S., Moriguchi, T., Kuida, K., Endo, J., Semba, K., Nishida, E. and Karasuyama, H. (1997). LOK is a novel mouse STE20-like protein kinase that is expressed predominantly in lymphocytes. *J. Biol. Chem.* **272,** 22679-22684.

Kyriakis, J. M. (1999). Signaling by the germinal center kinase family of protein kinases. *J. Biol. Chem.* **274,** 5259-5262.

Lehman, J. M., Riethmuller, G. and Johnson, J. P. (1990). Nck, a melanoma cDNA encoding a cytoplasmic protein consisting of Src homology units SH2 and SH3. *Nucl. Acids Res.* **18,** 1048.

Li, L., Yuan, H., Xie, W., Mao, J., Caruso, A. M., McMahon, A., Sussman, D. J. and Wu, D. (1999). Dishevelled proteins lead to two signaling pathways. Regulation of LEF- 1 and c-Jun N-terminal kinase in mammalian cells. *J. Biol. Chem.* **274,** 129-134.

Liu, J. F., Chevet, E., Kebache, S., Lemaitre, G., Barritault, D., Larose, L. and Crepin, M. (1999). Functional Rac-1 and Nck signaling networks are required for FGF-2- induced DNA synthesis in MCF-7 cells. *Oncogene* **18,** 6425-6433.

Manser, E. and Lim, L. (1999). Roles of PAK family kinases. *Prog. Mol. Subcell Biol.* **22,** 115-133.

Martin, G. A., Bollag, G., McCormick, F. and Abo, A. (1995). A novel serine kinase activated by rac1/CDC42Hs-dependent autophosphorylation is related to PAK65 and STE20. *EMBO J.* **14,** 1970-1978.

Martin, J. H., Mohit, A. A. and Miller, C. A. (1996). Developmental expression in the mouse nervous system of the p493F12 SAP kinase. *Brain Res. Mol. Brain Res.* **35,** 47-57.

Mlodzik, M. (1999). Planar polarity in the Drosophila eye: a multifaceted view of signaling specificity and cross-talk. *EMBO J.* **18,** 6873-6879.

Mortensen, R. M., Conner, D. A., Chao, S., Geisterfer-Lowrance, A. A. and Seidman, J. G. (1992). Production of homozygous mutant ES cells with a single targeting construct. *Mol. Cell Biol.* **12,** 2391-2395.

Noselli, S. (1998). JNK signaling and morphogenesis in Drosophila. *Trends Genet.* **14,** 33-38.

Paricio, N., Feiguin, F., Boutros, M., Eaton, S. and Mlodzik, M. (1999). The Drosophila STE20-like kinase misshapen is required downstream of the Frizzled receptor in planar polarity signaling. *EMBO J.* **18,** 4669-78.

Pawson, T. and Nash, P. (2000). Protein-protein interactions define specificity in signal transduction. *Genes Dev.* **14,** 1027-1047.

Pombo, C. M., Kehrl, J. H., Sanchez, I., Katz, P., Avruch, J., Zon, L. I., Woodgett, J. R., Force, T. and Kyriakis, J. M. (1995). Activation of the SAPK pathway by the human STE20 homologue germinal centre kinase. *Nature* **377,** 750-754.

Pombo, C. M., Tsujita, T., Kyriakis, J. M., Bonventre, J. V. and Force, T. (1997). Activation of the Ste20-like oxidant stress response kinase-1 during the initial stages of chemical anoxia-induced necrotic cell death. Requirement for dual inputs of oxidant stress and increased cytosolic [Ca^{2+}]. *J. Biol. Chem.* **272,** 29372-29379.

Riesgo-Escovar, J., Hafen, E. (1997a). Drosophila Jun kinase regulates expression of decapentaplegic via the ETS-domain protein Aop and the AP-1 transcription factor DJun during dorsal closure. *Genes Dev.* **11,** 1717-1727.

Riesgo-Escovar, J. R., Jenni, M., Fritz, A., Hafen, E. (1996). The Dorsophila Jun-N-terminal kinase is required for cell morphogenesis but not for DJun-dependent cell fate specification in the eye. *Genes Dev.* **10,** 2759-2768.

Riesgo-Escovar, J. R. and Hafen, E. (1997b). Common and distinct roles of DFos and DJun during drosophila development. *Science* **278,** 669-672.

Rockow, S., Tang, J., Xiong, W. and Li, W. (1996). Nck inhibits NGF and basic FGF induced PC12 cell differentiation via mitogen-activated protein kinase-independent pathway. *Oncogene* **12,** 2351-2359.

Ruan, W., Pang, P. and Rao, Y. (1999). The SH2/SH3 adaptor protein dock interacts with the Ste20-like kinase misshapen in controlling growth cone motility. *Neuron* **24,** 595-605.

Schlaeger, T. M., Bartunkova, S., Lawitts, J. A., Teichmann, G., Risau, W., Deutsch, U. and Sato, T. N. (1997). Uniform vascular-endothelial-cell-specific gene expression in both embryonic and adult transgenic mice. *Proc. Natl. Acad. Sci. USA* **94,** 3058-3063.

Schlaepfer, D. D., Broome, M. A. and Hunter, T. (1997). Fibronectin-stimulated signaling from a focal adhesion kinase-c-Src complex:

involvement of the Grb2, p130cas, and Nck adaptor proteins. *Mol. Cell Biol.* **17,** 1702-1713.

Schlessinger, J. (1994). SH2/SH3 signaling molecules. *Curr. Opin. Genet. Dev.* **4,** 25-30.

Sieg, D. J., Hauck, C. R. and Schlaepfer, D. D. (1999). Required role of focal adhesion kinase (FAK) for integrin-stimulated cell migration. *J. Cell Sci.* **112,** 2677-2691.

Simeone, A., Acampora, D., Mallamaci, A., Stornaiuolo, A., D'Apice, M. R., Nigro, V. and Boncinelli, E. (1993). A vertebrate gene related to orthodenticle contains a homeodomain of the bicoid class and demarcates anterior neuroectoderm in the gastrulating mouse embryo. *EMBO J.* **12,** 2735-2747.

Sluss, H. K., Han, Z., Barrett, T., Davis, R. J. and Ip, Y. T. (1996). A JNK signal transduction pathway that mediates morphogenesis and an immune response in Drosophila. *Genes Dev*. **10,** 2745-2758.

Song, D. L., Chalepakis, G., Gruss, P. and Joyner, A. L. (1996). Two Pax-binding sites are required for early embryonic brain expression of an Engrailed-2 transgene. *Development* **122,** 627-635.

Su, Y. C., Han, J., Xu, S., Cobb, M. and Skolnik, E. Y. (1997). NIK is a new Ste20-related kinase that binds NCK and MEKK1 and activates the SAPK/JNK cascade via a conserved regulatory domain. *EMBO J.* **16,** 1279-1290.

Su, Y. C., Maurel-Zaffran, C., Treisman, J. E. and Skolnik, E. Y. (2000). The ste20 kinase misshapen regulates both photoreceptor axon targeting and dorsal closure, acting downstream of distinct signals. *Mol. Cell Biol.* **20,** 4736-4744.

Su, Y. C., Treisman, J. E. and Skolnik, E. Y. (1998). The Drosophila Ste20-related kinase misshapen is required for embryonic dorsal closure and acts through a JNK MAPK module on an evolutionarily conserved signaling pathway. *Genes Dev.* **12,** 2371-2380.

Sun, X., Meyers, E. N., Lewandoski, M. and Martin, G. R. (1999). Targeted disruption of Fgf8 causes failure of cell migration in the gastrulating mouse embryo. *Genes Dev.* **13,** 1834-1846.

Swiatek, P. J., Lindsell, C. E., del Amo, F. F., Weinmaster, G. and Gridley, T. (1994). Notch1 is essential for postimplantation development in mice. *Genes Dev.* **8,** 707-19.

Takada, S., Stark, K. L., Shea, M. J., Vassileva, G., McMahon, J. A. and McMahon, A. P. (1994). Wnt-3a regulates somite and tailbud formation in the mouse embryo. *Genes Dev.* **8,** 174-189.

Tam, P. P. and Behringer, R. R. (1997). Mouse gastrulation: the formation of a mammalian body plan. *Mech. Dev.* **68,** 3-25.

Tam, P. P. and Trainor, P. A. (1994). Specification and segmentation of the paraxial mesoderm. *Anat. Embryol. (Berl)* **189,** 275-305.

Tybulewicz, V. L., Crawford, C. E., Jackson, P. K., Bronson, R. T. and Mulligan, R. C. (1991). Neonatal lethality and lymphopenia in mice with a homozygous disruption of the c-abl proto-oncogene. *Cell* **65,** 1153-1163.

Wilkinson, D. G., Bhatt, S. and Herrmann, B. G. (1990). Expression pattern of the mouse T gene and its role in mesoderm formation [see comments]. *Nature* **343,** 657-659.

Yamaguchi, T. P., Harpal, K., Henkemeyer, M. and Rossant, J. (1994). fgfr-1 is required for embryonic growth and mesodermal patterning during mouse gastrulation. *Genes Dev.* **8,** 3032-3044.

Yamaguchi, T. P., Takada, S., Yoshikawa, Y., Wu, N. and McMahon, A. P. (1999). T (Brachyury) is a direct target of Wnt3a during paraxial mesoderm specification. *Genes Dev.* **13,** 3185-3190.

Yoshikawa, Y., Fujimori, T., McMahon, A. P. and Takada, S. (1997). Evidence that absence of Wnt-3a signaling promotes neuralization instead of paraxial mesoderm development in the mouse. *Dev. Biol.* **183,** 234-242.